Proceedings of the Canadian Society for Mechanical Engineering International Congress
32nd Annual Conference of the Computational Fluid Dynamics Society of Canada
Canadian Society of Rheology Symposium
CSME/CFDSC/CSR 2025
May 25–28, 2025, Montréal, Québec, Canada

NUMBER

Numerical analysis of partial charging effect in a latent heat thermal energy storage unit.

Soumaya Sokakini[1]*, Jules Voguelin Simo Tala[1], Lionel Nadau[2], Adrian Ilinca[3] Daniel Bougeard[1]

[1]IMT Nord Europe, Institut Mines-Telecom, Univ. Lille, Centre for Energy and Environment, F-59000 Lille, France
[2]ENGIE Lab CRIGEN, 4 rue Joséphine Baker, 93240 Stains, France
[3]Department of Mechanical Engineering, École de Technologie Supérieure, Montreal, QC H3C 1K3, Canada
*soumaya.sokakini@imt-nord-europe.fr

March 27, 2025

***Abstract*—The present study focuses on the analysis of the partial charging as an operating condition of a finned multitube latent heat thermal energy storage unit, and aims to investigate its impact on the thermal performances. To this end, partial charge with 80% total melting and full charge with totally melted phase change material (PCM) are compared, firstly during the charging process and then during the subsequent complete discharge process. Phase change duration and stored/released energy are chosen as performance indicators for this study. The phase change is modeled in 3D using the enthalpy-porosity method. The results show that stopping the charging process at a level of charge of 80% saves a significant charging time, 39.83%, with a corresponding unexploited energy of only 25.48%. However, for the subsequent discharge process, after partially charging the storage unit, the time reduction is not significant with only 12.4%, for an equivalent energy reduction of 25.8%. Furthermore, the solid volume fraction contours of the PCM during the phase change process show that the residual solid PCM from the charging process continues to melt during the discharging period, thereby changing the phase change front compared to the case after full charging.**

***Keywords-component*—Partial charge, full charge, latent heat storage, phase change material.**

I. INTRODUCTION

In a context of energy transition and energy efficiency optimization, thermal storage plays a key role in managing energy resources, reducing dependence on fossil fuels and minimizing CO_2 emissions. As a storage technology, latent heat storage stands out for its high energy density and its ability to store and release heat at quasi-constant temperature, making it particularly attractive. A number of studies have therefore been carried out, including on environmental and economic feasibility [1],[2], phase change material (PCM) selection and characterization blue[3],[4], while most of them focused on addressing the low PCM conductivity issue through various heat transfer enhancement techniques [5],[6],[7]. Nevertheless, the large majority of these studies are carried out on complete charge-discharge cycles, neglecting partial charge-discharge scenarios, which can be of great interest and are sometimes unavoidable. In fact, allowing partial charging and discharging of the storage unit increases its flexibility and enables adaptation to fluctuating demands and to varying available quantities of thermal heat to be stored.

Among the few studies on partial charge/discharge operating conditions, Gasia et al. [8] evaluated, through an experimental study, the effect of the RAS (Ratio of Accumulated Energy) on the performance of a shell and tube latent heat energy storage (LHTES) unit, and this, by comparing five different RAS comprised between 58% and 97%. Their results revealed that partial charge of 85% or more of the system's maximum energy capacity is an good option, providing that a maximum 10% reduction in discharge heat transfer rates is allowed. The same research group [9] investigated later the impact of the stand-by period between charging and discharging process, by testing three different periods : 25, 60 and 120 min, and working under partial load with different states of charge. They concluded that overall, the stand-by period has no significant influence on the subsequent discharge process. Arena et al. [10] performed a numerical study to assess the effect of partial charge on the charging process itself and the following discharge, based on four different states of charge

Financial support : ENGIE SA and the Haut-de-France region (HDF)

ranging from 100% to 75%. They found that interrupting the charging process at a liquid fraction between 0.75 and 0.90 can reduce charging time by up to 30-50%, with a corresponding reduction in unused storage capacity of around 15-30%. Zauner et al. [11] experimentally compared the discharge of a fully and partially charged multitube storage unit. Quite similar power and outlet temperature behaviors were observed for both operating conditions. They also performed a series of partial charge and discharge cycles, and their results showed fluctuating PCM temperature, power and energy profiles. Scharinger-Urschitz et al. [12] assessed the performance of a finned LHTES unit for partial charge and discharge cycles with different states of charge, with particular focus on power rates. Their results revealed that the proposed finned LHTES unit exhibits high power rates for all partial and full charge/discharge states compared with the finless LHTES unit. In their numerical study, McKenna et al. [13] investigated whether partial load can improve the overall performance of an LHTES unit integrated into an HVAC system in a commercial office building. They concluded that fully charging the LHTES unit is non-optimal as the efficiency sharply drops below 20% charge and the charging rate decreases above 10%. In addition, the efficiency of subsequent full discharge was found to decrease with increasing initial charge fraction. D'Avignon et al. [14] studied the behavior of commercial slab-like PCM capsules under different operating conditions. Their results indicated that interrupting the charge and discharge alters the phase change temperature. Bédécarats et al. in [15] and [16] examined the effect of the discharge process. Their numerical and experimental studies using encapsulated PCM showed that partial discharge increased the phase change temperature of the following charge process.

From literature review, it can be noticed that, despite its importance, partial charge and discharge remains under-explored. Therefore, based on a 3D numerical approach, the present study aims to provide more insights into how partial charging affects the performance of an enhanced LHTES unit with multitubes and fins, including both the charging process itself as well as the following discharge. Moreover, this study focuses not only on the global scale, but also on the local scale by analyzing the solid volume fraction contours, thus providing a better understanding of the phenomena involved in partial-load operating conditions.

II. Physical Model

The present study is carried out on a finned multitube latent heat thermal energy storage unit (FM-LHTES), represented in fig. 1. It consists of a horizontal, cylindrical shell-and-tube heat exchanger in which the heat transfer fluid flows through four tubes, while the shell contains the PCM. The tubes are 2 cm inner diameter and 2 mm thick, equidistantly placed at 5 cm from the centre of the shell. The 70 length shell has an inner diameter of 14.6 cm and a thickness of 2 mm. In addition to extending the heat exchange surface through the use of multiple tubes, and to further enhance heat transfer in the storage unit, 2mm thick cross-shaped fins are used to interconnect the tubes and the shell. These fins, , tubes and the shell are made of aluminium. Furthermore, erythritol is used as PCM and hytherm 600 as heat transfer fluid (HTF). The thermophysical properties of the different materials are summarised in table I.

For symmetry reasons, only half of the geometry is simulated in this study, thereby reducing the calculation time and cost.

III. Methodology

The assessment of partial charge of the FM-LHTES unit is performed through the comparison of two scenarios. In the first case, the thermal storage unit is assumed to be at first fully charged, then is fully discharged, while in the second case, it is considered to be at first, partially charged to 80%, then is completely discharged. The level of charge/discharge is defined by the liquid volume fraction, with full and partial charge corresponding to LVF= 1 and LVF=0.8 respectively, and a full discharge to LVF=0. It should be noted that for this study, the discharge is initiated directly after the charging process, without any transition period (stand-by period).

IV. Mathematical and Numerical Model

The mathematical model is based on the Naviers-Stockes equations associated with the enthalpy-porosity method [17], which is very often used to model solid-liquid phase change problems. To simplify the problem resolution, some assumptions are made: HTF and PCM are considered incompressible with laminar flow. Moreover, volume expansion, heat loss and viscous dissipation are neglected. Furthermore, the Boussinesq approximation is considered to account for natural convection. The governing equations are then described as follows:

Mass conservation equation

$$\nabla \cdot \vec{V} = 0 \tag{1}$$

Momentum conservation equation

$$\rho \frac{\partial \vec{V}}{\partial t} + \rho \left(\vec{V} \cdot \nabla \right) \vec{V} = -\nabla P + \mu \nabla^2 \vec{V} + \rho \vec{g} \beta \left(T_{ref} - T \right) + A \vec{V} \tag{2}$$

With $A = -C \frac{(1-f_l)^2}{f_l^3 + \epsilon}$, and the mushy zone constant C is taken as 10^6.

Energy equation

$$\rho \frac{\partial H}{\partial t} + \rho \nabla \left(\vec{V} \cdot H \right) = \nabla \left(\frac{\lambda}{C_p} \nabla h \right) \tag{3}$$

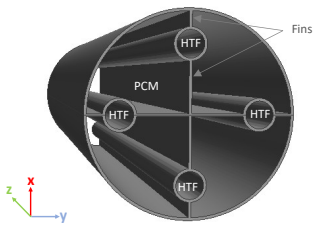

Figure. 1. 3D illustration of the finned multitube storage unit.

TABLE. I
THERMOPHYSICAL PROPERTIES OF PCM (ERYTHRITOL), HTF (HYTHERM 600) AND ALUMINUM [18],[19].

	ρ	μ	λ	C_p	L	T_s	T_l	β
	kg.m^{-3}	Pa.s	$W.m^{-1}.K^{-1}$	$J.kg^{-1}.K^{-1}$	$kJ.kg^{-1}$	$°C$	$°C$	K^{-1}
PCM	1480 at 20 °C	0.01	0.733 at 20°C 0.326 at 140°C linear	solid : 1380 liquid : 2760 linear between T_s and T_l	339.8	116.7	118.7	0.001014
HTF	720.9	19.5×10^{-3}	0.1161	3097.4	-	-	-	-
Aluminum	2719	-	202.4	871	-	-	-	-

With

$$H = h + \Delta H \tag{4}$$

$$h = h_{ref} + \int_{T_{ref}}^{T} C_p dT \tag{5}$$

$$\Delta H = f_l \cdot L \tag{6}$$

With f_l is the PCM liquid volume fraction defined as :

$$f_l = \begin{cases} 0 & \text{if } T < T_s \\ \dfrac{T - T_s}{T_l - T_s} & \text{if } T_s < T < T_l \\ 1 & \text{if } T > T_l \end{cases} \tag{7}$$

A. Initial and boundary conditions

- Charge process

As initial condition and for both cases, the entire domain system, including HTF, PCM, shell, tubes and fins, is assumed to be at a constant temperature T(x,y,z)=80°C. For the boundary conditions, a constant temperature of 150°C and a Poiseuille velocity profile with an bulk velocity of 2.7 m/s are imposed at the HTF inlet. At the outlet, a pressure boundary condition is applied. The outer surface of the shell is considered to be adiabatic, thus neglecting heat loss to the environment. The solid-solid and solid-fluid interfaces are treated with conjugate heat transfer condition. In addition, symmetry boundary condition is applied at the vertical mid-plane of the storage unit.

- Discharge process

For the discharge process, the end state of the previous charge process (partial or complete) is taken as initial condition. In addition, all the boundary conditions are retained as for the charging process, apart from the HTF inlet temperature, which is equal to 80°C.

B. Grid and step time sensitivity analysis

The governing equations were solved in 3D using the commercial CFD code STAR CCM+. A grid sensitivity analysis was performed by generating five grids numbers, ranging from 1 million to 4.3 million cells. Simulation results during the discharge process, including solid volume fraction, heat duty and friction factor, were compared for the different cell numbers to the finest grid with 4.3 million cells. Fig. 2 shows the evolution of the heat duty over time for the different cell numbers along with their relative error with respect to the finest grid. According to the obtained results, the 2.7 million-cell grid was chosen, balancing computational cost and numerical accuracy, with a relative error of less than 1%.

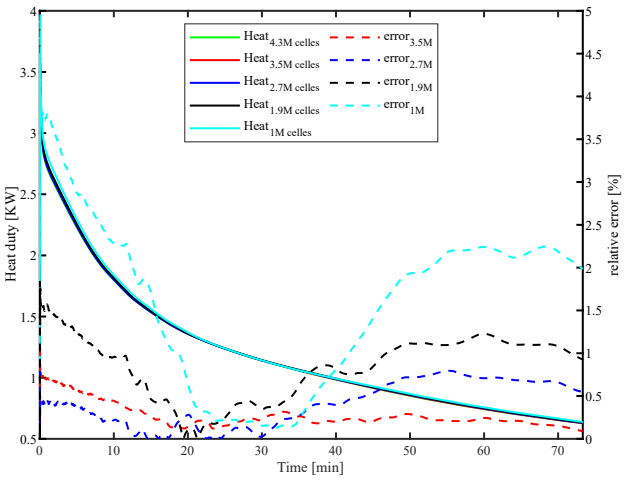

Figure. 2. Transient evolution of energy during charge and discharge cycle with partial and full charge cases.

Using this mesh topology, a time-step sensitivity analysis was subsequently carried out, involving six time steps: 0.025s, 0.05s, 0.1s, 0.2s, 0.4s and 0.8s. It was observed that at the start of the discharge process, a small time step is required, which is due to the high temperature gradient in the early stages. Then, as the process progresses, the time step can be progressively increased, while maintaining good accuracy.Hence a variable time step is opted for, with $\Delta t = 0.025s$ for $0s < t \leq 100s$, $\Delta t = 0.05s$ for $100s < t \leq 150s$, $\Delta t = 0.2s$ for $150s < t \leq 250s$ and $\Delta t = 0.4s$ for $t > 250s$.

V. RESULTS AND ANALYSIS

A. Global analysis

This section aims to quantify the influence of the partial charging on the global performance of the FM-LHTES unit. For this purpose, partial charge (LVF=0.8) will be compared with full charge operating condition (LVF=1), with particular emphasis on two key parameters: the time saving and the associated unused energy. In addition, as partial discharge can have an impact not only on the charging process itself, but also on the following discharge process, both processes

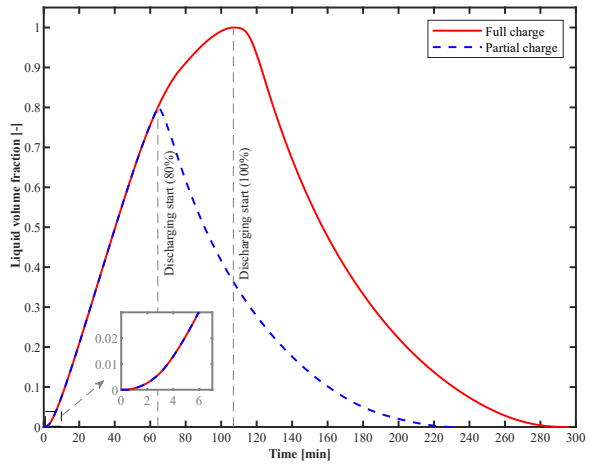

Figure. 3. Transient evolution of liquid volume fraction during charge and discharge cycle with partial and full charge cases.

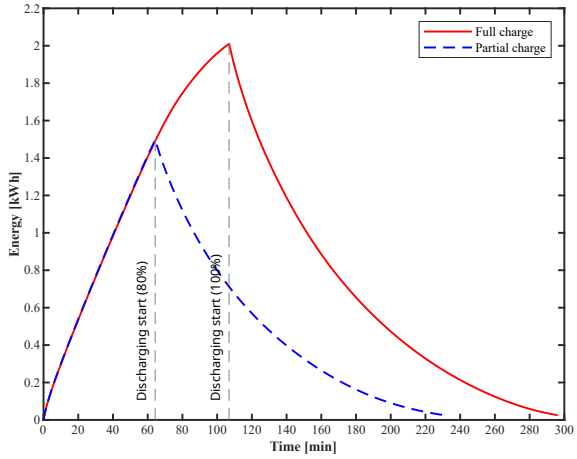

Figure. 4. Transient evolution of energy during charge and discharge cycle with partial and full charge cases.

will be analysed.

Fig. 3 and Fig. 4 show respectively the evolution over time of the liquid volume fraction and the energy stored/released during the charge-discharge cycle. The dotted blue line denotes partial charge and the solid red line full charge. Furthermore, the energy represented is that contained in the PCM as well as in the metallic regions , and it is calculated as the integral of the heat flux over the process period.

1) Charging process

During the charging process, due to heat exchange with the hot HTF, the solid PCM melts and transforms from solid to liquid state, leading to an increase in the liquid volume fraction in Fig. 3. The graph analysis shows that during the first few minutes, the evolution of the liquid volume fraction is relatively slow, which is due to the increase in PCM temperature up to the melting point and to conduction being the principal heat transfer mode during this first melting phase. Then, once natural convection develops and intensifies, the melting process becomes faster and the liquid volume fraction follows a quasi-linear evolution. However, at advanced stages (around 80%), the curve's slope gradually decreases, signifying that the remaining solid PCM requires longer time to melts. This is due to the small temperature gradient between the PCM and the HTF in the latter stages.
The analysis of the liquid volume fraction shows that it takes 106.87 min (1h47 min) for the PCM to be completely melted, however, stopping the charging process at a state of charge of 80% reduces this time to 64.3 min (1h4min). Therefore, by partially charging the storage unit, 43 minutes were saved, corresponding to 39.8% of the complete charge time. These results show that partial discharge is relevant in terms of charging time, however this is not enough to conclude about the pertinence of partial charging, as the associated energy loss must be also quantified.

During this charging phase, the energy is absorbed and stored in the PCM in latent and sensible forms as well as in the metal parts, which is reflected by an increase in the energy curve in Fig. 4. The comparison between full and partial charge indicates that in the first scenario, a total of 2.01 kWh is stored, compared with 1.49 kWh in the second. This represents 25.48% of the unstored energy, contained in the non-melted PCM in latent form as well as in the already melted PCM in sensible form, due to the elevation of its temperature.

2) Discharging process

After examining the effect of partial charging on the FM-LHTES unit during the charging process, this section examines its impact on the subsequent discharging process.
To discharge the storage unit, the HTF is introduced at a temperature below the PCM's melting temperature and, due to the heat exchange between these two, the PCM changes phase from liquid to solid, resulting in a decrease in the liquid volume fraction, as it can be observed in Fig. 3.
The comparison of the discharge time between the scenarios after a full and partial charge indicates, as expected, that the discharge is faster after partial charge. The reason for this is that, in this case, the amount of PCM to be solidified is smaller, since some regions are already solid remaining from the prior charging process. In fact, following partial load at 80%, the PCM takes 165.6 min (2h45min) to completely solidifies compared with 189.1 min (3h9min) after a complete charge. This means that only 12.4% of the discharge time is saved.

From an energetic standpoint, the PCM during the discharge process releases the energy previously stored, and this is represented by a descending curve in Fig. 4. Besides, the results show that after a full charge, 1.98 kwh is released, compared with 1.47 kwh when the discharging process starts

after an interruption of the charging process at 80%. This equates to a 25.8% reduction in the energy involved, which is greater than the associated time reduction of 12.4%.

B. Local analysis

For a more in-depth analysis of the impact of partial discharge, particularly on the subsequent charging process, the melting or solidification front evolution of the two scenarios studied will be compared in this section.

Fig. 5 depicts the contours of the solid volume fraction in the central section of the FM-LHTES (z=L/2) for discharge following partial loading (a) and full loading (b). For a more accurate comparison, the two cases are compared at the solidification rate, i.e. at the beginning, at 24%, 28%, 44%, 55%, these percentages are relative to the complete discharge defined by the solidification of the totality of the PCM in this central plane. The red color refers to the solid PCM, the blue to liquid phase and the other colors to the mushy zone.

At the initial stage of the discharge process, all the PCM is in liquid phase after a full charge. However, in the other scenario, there is still some solid PCM, most of which is in the lower part of the FM-LHTES unit. This is the consequence of natural convection during the previous charge which, due to the difference in density, raises the liquid PCM to the top and the solid to the bottom, resulting in slower melting in the lower part. As time goes by, the PCM begins to solidify in both cases, firstly around the tubes and fins. Furthermore, in the scenario after partial discharge, alongside the PCM solidification, the remaining solid PCM from the prior charging process continues to melt due to heat exchange with the neighbouring hot PCM. This is most visible in the lower section, where by comparing the discharge start with 28%, it can be seen that the red areas become smaller. Then, once the solidification front reaches these areas of the remaining solid PCM (44%), it merges with them and this continuous melting phenomenon stops.

The solid volume fraction contours clearly demonstrate that this double phase change front (solidification + continuing melting) affects the overall solidification front shape. After a full charge, the solidification front is almost symmetrical, due to heat transfer by conduction, whereas this is not the case after a partial charge where more liquid PCM appears in the upper part.

VI. Conclusion

The effect of partial charging on the performance of a finned multitube latent heat thermal energy storage unit was investigated in the present work. Performance was evaluated separately during the charging and discharging process through comparison of a full charge-discharge cycle and an 80% (LVF=0.8) charge and full discharge (LVF=0) cycle. The following conclusions can be made :

- Melting the remaining 20% takes a considerable amount of time, and stopping the charging process at a level of charge of 80% (LVF=0.8) saved 39.8% charging time, with an associated unstored energy of only 25.48%.
- When starting the discharge process after an 80% partial charge, the time required to fully discharge (solidify) the storage unit is shortened by only 12.4%, with a corresponding 25.8% reduction in discharged energy. As a result, the partial-charge operating mode is more advantageous during the charging process than during subsequent discharge.
- The evolution of the phase change front during the discharge process is affected by the previous partial charge, and is characterized by a double melting/solidification front, i.e. solidification and continuing melting of the remaining solid PCM from the previous charging process.

Acknowledgment

This research was financially supported by ENGIE SA and the Haut-de-France region (HDF), to whom we extend our sincere gratitude.

References

[1] S. Mazzoni, J.Y. Sze, B. Nastasi, S. Ooi, U. Desideri and A. Romagnoli, "A techno-economic assessment on the adoption of latent heat thermal energy storage systems for district cooling optimal dispatch operations", Applied Energy, vol. 289, p. 116646, May. 2021.

[2] E. Gholamian,V. Zare, N. Javani and F. Ranjbar, "Dynamic 4E (energy, exergy, economic and environmental) analysis and tri-criteria optimization of a building-integrated plant with latent heat thermal energy storage", Energy Conversion and Management, vol. 267, p. 115868, September. 2022.

[3] X. Yu, J. Chang, R. Huang, Y. Huang, Y. Lu, Z. Li et al. "Sensitivity analysis of thermophysical properties on PCM selection under steady and fluctuating heat sources: A comparative study", Applied Thermal Engineering, vol. 186, p. 116527, March. 2021.

[4] N. Soares, T. Matias, L. Durães , P.N. Simões and J.J. Costa, "Thermophysical characterization of paraffin-based PCMs for low temperature thermal energy storage applications for buildings", Energy, vol. 269, p. 126745, April. 2023.

[5] A. Kaboré, J.V. Simo Tala, Z.Younsi and D. Bougeard, "Numerical analysis and optimization of the heat transfer enhancement from the heat transfer fluid side in a shell-and-tube latent heat thermal energy storage unit: Application to buildings thermal comfort improvement", Energy storage, vol. 74, p. 109530, December. 2023.

[6] S. Lu, Q. Lin, B. Xu, L. Yue and W. Feng, "Thermodynamic performance of cascaded latent heat storage systems for building heating", Energy, vol. 282, p. 128752, November. 2023.

[7] X. Hu, X. Gong, F. Zhu,X. Xing, Z. Li and X. Zhang, "Thermal analysis and optimization of metal foam PCM-based heat sink for thermal management of electronic devices", Renewable energy, vol. 212, p. 227-237, August. 2023.

[8] J. Gasia, A. De Gracia, G. Peiró, S. Arena, G. Cau and L. F. Cabeza, "Use of partial load operating conditions for latent thermal energy storage management", Applied Energy, vol. 216, p. 234-242, April. 2018.

[9] J. Gasia, A. De Gracia, G. Zsembinszki, and L. F. Cabeza, "Influence of the storage period between charge and discharge in a latent heat thermal energy storage system working under partial load operating conditions", Applied Energy, vol. 235, p. 1389-1399, February. 2019.

[10] S. Arena, E. Casti, J. Gasia, L. F. Cabeza, and G. Cau, "Numerical analysis of a latent heat thermal energy storage system under partial load operating conditions", Renewable Energy, vol. 128, p. 350-361, December. 2018.

[11] C. Zauner, F. Hengstberger, B. Mörzinger, R. Hofmann, and H. Walter,"Experimental characterization and simulation of a hybrid sensible-latent heat storage", Applied Energy, vol. 189, p. 506-519, March. 2017.

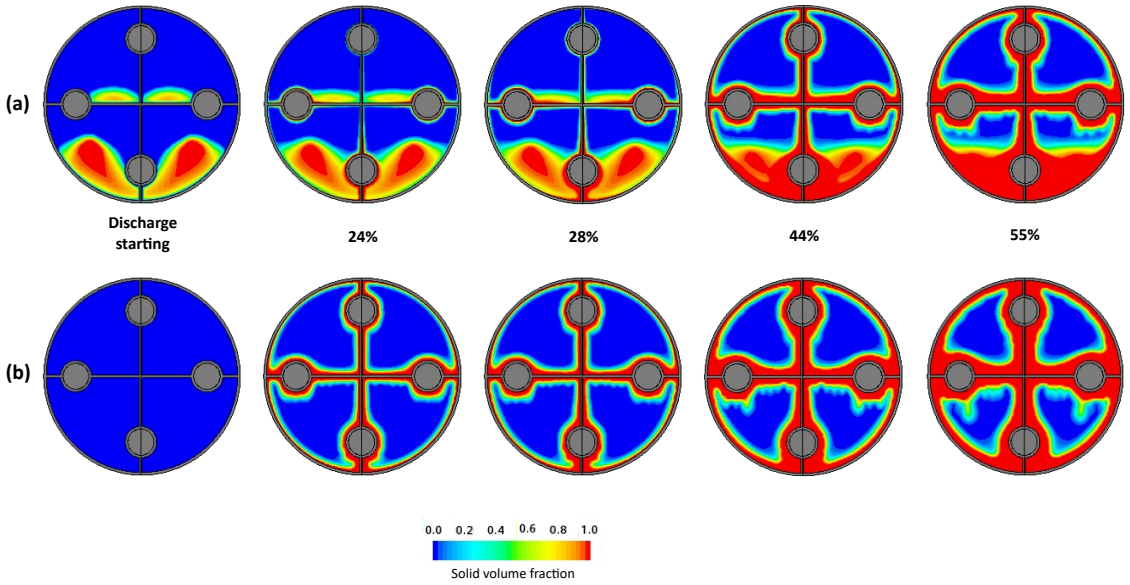

Figure. 5. Solid volume fraction contours at different state of discharge after partial charge (a) and after complete charge (b).

[12] G. Scharinger-Urschitz, P. Schwarzmayr, H. Walter, and M. Haider,"Partial cycle operation of latent heat storage with finned tubes", Applied Energy, vol. 280, p. 115893, December. 2020.

[13] P. McKenna, W.J.N. Turner and D.P. Finn, "Thermal energy storage using phase change material: Analysis of partial tank charging and discharging on system performance in a building cooling application", Applied Thermal Engineering, vol. 198, p. 117437, November. 2021.

[14] K. D'Avignon and M. Kummert, "Experimental assessment of a phase change material storage tank", Applied Thermal Engineering, vol. 99, p. 880-891, April. 2016.

[15] J. P. Bédécarrats, J. Castaing-Lasvignottes, F. Strub, and J. P. Dumas, "Study of a phase change energy storage using spherical capsules. Part I: Experimental results", Energy Conversion and Management, vol. 50, n 10, p. 2527-2536, October. 2009.

[16] J. P. Bédécarrats, J. Castaing-Lasvignottes, F. Strub, and J. P. Dumas, "Study of a phase change energy storage using spherical capsules. Part II: Numerical modelling", Energy Conversion and Management, vol. 50, n 10, p. 2537-2546, October. 2009.

[17] V. R. Voller, M. Cross, et N. C. Markatos, "An enthalpy method for convection/diffusion phase change", Numerical Meth Engineering, vol. 24, n 1, p. 271-284, January. 1987.

[18] A. J. Parry, P. C. Eames, and F. B. Agyenim, "Modeling of Thermal Energy Storage Shell-and-Tube Heat Exchanger", Heat Transfer Engineering, vol. 35, n 1, p. 1-14, January. 2014.

[19] A. K. Raul, P. Bhavsar, et S. K. Saha, "Experimental study on discharging performance of vertical multitube shell and tube latent heat thermal energy storage", Journal of Energy Storage, vol. 20, p. 279-288, December. 2018.

NOMENCLATURE

C_p	Specific heat capacity ($J.kg^{-1}.K^{-1}$)
f_l	liquid volume fraction ($-$)
h	Sensible enthalpy per unit mass ($J.kg^{-1}$)
g	Gravity acceleration ($m.s^{-2}$)
H	Total enthalpy per unit mass ($J.kg^{-1}$)
L	Latent heat ($J.kg^{-1}$)
t	Time (s)
T	Temperature ($°C$)
$\vec{V}$	Velocity vector ($m.s^{-1}$)
P	Pressure (Pa)

Greek symbols

β	Thermal expansion coefficient (K^{-1})
ϵ	Numerical coefficient ($-$)
λ	Thermal conductivity ($W.m^{-1}.K^{-1}$)
μ	Dynamic viscosity ($Pa.s$)
ρ	Density ($kg.m^{-3}$)

Subscripts

ref	Reference
l	Liquidus
s	Solidus

Abbreviations

HTF	Heat Transfer Fluid
PCM	Phase Change Material
LVF	Liquid Volume Fraction
CFD	Computational Fluid Dynamics
LHTES	Latent Heat Thermal Energy Storage
FM-LHTES	Finned Mutitube Latent Heat Thermal Energy Storage